Electronic Journal of Biotechnology 82 (2026) 100716

Contents lists available at ScienceDirect

Electronic Journal of Biotechnology

journal homepage: www.elsevier.com/locate/ejbt

Research article

Surfactant protein D regulates Notch activity for secretory cell repair and regeneration to prevent post-acute pancreatitis diabetes ☆

Jiexin Yan, Shuxiong Liu, Jian He *

Department of Emergency, The Third Affiliated Hospital of Naval Medical University, Shanghai, China

GRAPHICAL ABSTRACT

Surfactant protein D regulates Notch activity for secretory cell repair and regeneration to prevent post-acute pancreatitis diabetes.

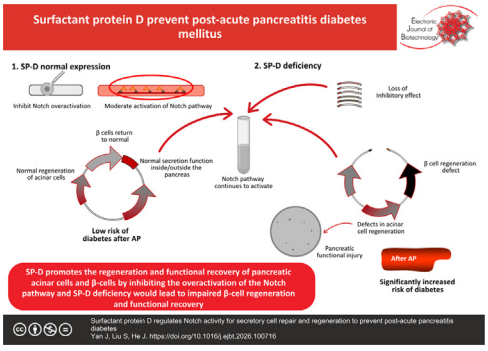

ARTICLE INFO

Article history:
Received 11 October 2025
Accepted 30 January 2026
Available online 14 May 2026

Keywords:
Acute pancreatitis (AP)
Glucose intolerance
Glucose metabolism
Insulin secretion
Notch signaling pathway
Pancreatic endocrine dysfunction
Pancreatic regeneration
SP-D knockout mice

ABSTRACT

Background: Pancreatic endocrine dysfunction following acute pancreatitis (AP) can lead to glucose intolerance and even diabetes. Surfactant protein D (SP-D), as an immune regulatory molecule, has not yet been clarified whether it participates in the regeneration of pancreatic acinar cells and β-cells by modulating the Notch pathway, thereby improving abnormal glucose metabolism. This study aimed to elucidate the role and mechanism of SP-D in promoting the regeneration of pancreatic secretory cells following AP and preventing post-pancreatitis diabetes by regulating the activity of the Notch pathway. *Results:* Using wild-type and SP-D gene knockout ($SP\text{-}D^{-/-}$) mice as models, dynamic observations were made after AP induction by Cerulein. Western blot analysis of pancreatic tissue revealed that in the $SP\text{-}D^{-/-}$-AP group (DG), the key Notch pathway molecules NICD and Hes1 were persistently upregulated; the expression of acinar cell regeneration marker SOX9 and β-cell precursor differentiation marker NGN3 was reduced, and the recovery of the β-cell function marker insulin was delayed. Glucose metabolism testing revealed that the DG had significantly elevated fasting blood glucose (7.6 ± 0.5 mmol/L) at 30 d

☆ Audio abstract available in Supplementary material.

* Corresponding author.
E-mail address: yanjiexin1993@163.com (J. He).

https://doi.org/10.1016/j.ejbt.2026.100716

Surfactant protein D (SP-D)
β-cell regeneration

and an increased area under the curve in the oral glucose tolerance test. Sustained elevation of serum amylase and insufficient insulin secretion were observed, along with a markedly delayed repair process. *Conclusions:* SP-D promotes the regeneration and functional recovery of pancreatic acinar cells and β-cells by inhibiting the overactivation of the Notch pathway, thereby improving abnormal glucose metabolism following AP.

How to cite: Yan J, Liu S, He J. Surfactant protein d regulates Notch activity for secretory cell repair and regeneration to prevent post-acute pancreatitis diabetes. Electron J Biotechnol 2026;82. https://doi.org/10.1016/j.ejbt.2026.100716.

1. Background

The pathological process of acute pancreatitis (AP) is characterized by acute acinar cell necrosis and severe inflammatory reactions caused by the abnormal activation of pancreatic enzymes, which not only leads to local pancreatic tissue damage but also causes long-term impairment of pancreatic exocrine and endocrine functions [1]. Its pathogenesis is closely related to the abnormal activation of trypsinogen within acinar cells, where activated pancreatic enzymes trigger autodigestion, destroying pancreatic parenchyma and surrounding tissues, while inducing the release of large amounts of inflammatory factors that form an inflammatory storm, further exacerbating tissue necrosis. Some patients still suffer from persistent endocrine dysfunction after recovery, eventually developing into post-pancreatitis diabetes, which seriously affects the quality of life [2]. It is currently widely believed in the academic community that the insufficient regenerative capacity of secretory cells after pancreatic injury is a key factor in this adverse outcome [3], with regeneration defects of acinar cells and β-cells being particularly prominent. After pancreatic injury, the body needs to go through a series of processes, such as necrotic tissue clearance, proliferation and differentiation of pancreatic stem cells, acinar ductal metaplasia (ADM), and β-cell regeneration, to achieve repair, and the obstruction of this repair process will directly lead to pancreatic function not recovering to normal levels.

The Notch pathway is a highly conserved signaling system in evolution, playing a core regulatory role in cell fate determination, stem cell maintenance, and tissue regeneration [4]. Studies have confirmed that the precise spatiotemporal regulation of Notch signaling is crucial for pancreatic development and regeneration after injury [5]. Moderately activated Notch signaling can maintain the state of pancreatic progenitor cells, promoting their proliferation and differentiation to participate in the repair process; however, overactivation can inhibit terminal cell differentiation, leading to impaired regeneration and repair [6]. In addition, recent studies have found that the Notch pathway can directly participate in the tissue repair process after pancreatitis by regulating the inflammatory microenvironment and the proliferation and differentiation of pancreatic progenitor cells [7], with its abnormal activity closely related to delayed pancreatic function recovery, providing an important direction for the study of pancreatitis repair mechanisms.

In recent years, the pulmonary innate immune molecule surfactant protein D (SP-D) has been found to be widely expressed in various extrapulmonary tissues, with significant immunomodulatory and tissue repair functions in addition to its classic host defense role [8]. SP-D can participate in maintaining tissue homeostasis by binding to pathogens and apoptotic cells to promote their clearance, regulating macrophage function, and inhibiting excessive inflammatory responses [9,10], with its regulatory role in inflammation-related diseases confirmed by multiple studies. Studies have suggested [11] that SP-D expression is abnormal in patients with AP and is associated with disease severity. In patients with severe AP complicated by acute respiratory distress syndrome, SP-D levels are significantly elevated, and after blood purification treatment, SP-D levels decrease, with improved patient prognosis, indicating that SP-D may be involved in the pathophysiological process of pancreatitis. However, whether SP-D directly participates in the repair process after pancreatic injury, especially whether it can affect the regeneration of acinar cells and β-cells by regulating Notch pathway activity, has not been systematically and deeply studied.

Based on the above research status, this study aims to explore the role of SP-D in pancreatic tissue repair after AP, focusing on clarifying whether it can promote the regeneration and functional recovery of acinar cells and β-cells by regulating the activity level of Notch, thereby improving abnormal glucose metabolism. It provides new molecular mechanisms and therapeutic strategies for preventing the occurrence of post-pancreatitis diabetes, filling the shortcomings in current research in this field.

2. Materials and methods

2.1. Experimental animals and grouping

SP-D gene knockout (SP-D^{-}/$^{-}$) mice (C57BL/6 background) were gifted by the Third Affiliated Hospital of Naval Medical University, and the genotype was identified by PCR (primer sequences: forward 5′-GCTGATGGGTGTAGGTGAAG-3′, reverse 5′-CAGGTGAGAT GACAGGAGAC-3′), ensuring a knockout efficiency of over 95%; wild-type (WT) C57BL/6 mice were purchased from Cyagen (Suzhou) Biosciences Inc. All mice were housed in the Third Affiliated Hospital of Naval Medical University SPF-grade animal facility with environmental conditions of temperature (22 ± 1)°C, humidity (55 ± 3)%, and a 12 h light/dark cycle (7:00–19:00 lighting), with standard feed and sterile water. The mice were acclimatized for 1 week before the experiment, and healthy male mice (8–10 weeks, 21 ± 1.5 g) were selected, excluding individuals with a body weight difference of more than 20%, listlessness, and organic lesions.

A completely randomized design was used to divide WT mice and SP-D^{-}/$^{-}$ mice into control (CON) and AP groups, respectively. Each group was further subdivided according to the observation time points (1, 3, 7, 30 d), with 10 mice included in each subgroup.

a. WT-CON group (AG): divided into WT-CON-1d/3d/7d/30d;
b. WT-AP group (BG): divided into WT-AP-1d/3d/7d/30d;
c. SP-D^{-}/$^{-}$-CON group (CG): divided into SP-D^{-}/$^{-}$-CON-1d/3d/7d/30d;
d. SP-D^{-}/$^{-}$-AP group (DG): divided into SP-D^{-}/$^{-}$-AP-1d/3d/7d/30d.

A total of 160 mice were included in the experiment, and all procedures were approved by the Third Affiliated Hospital of Naval Medical University Animal Ethics Committee.

2.2. Major reagents and instruments

The following major reagents and instruments were used. Cerulein (Sigma-Aldrich) was used for the induction of AP. Key antibodies

(Ab) included: NICD, Hes1 (Abcam), SOX9, NGN3, and Insulin (CST); β-actin Ab and HRP-conjugated secondary Ab were purchased from Beyotime Biotechnology. Protein quantification and gel preparation were performed using Thermo Fisher kits, and blood glucose, insulin, and amylase were detected using corresponding kits. The main instruments included a small animal blood glucose analyzer (Roche), a microplate reader, a Western blot (WB) electrophoresis and transfer system (Bio-Rad), an upright fluorescence microscope (Olympus), a paraffin microtome, and a tissue grinder.

2.3. Construction of the AP model

AP was induced in mice by intraperitoneal injection of Cerulein. Cerulein was dissolved in sterile saline to a concentration of 50 μg/mL and injected at 50 μg/kg, at hourly intervals, seven times in total, with an injection volume of no more than 0.2 mL per mouse; the control group received an equal volume of sterile saline. The condition of the mice was closely monitored during the modeling process, and the experiment was immediately terminated and recorded as a modeling failure if persistent convulsions, rapid breathing (>100 times/min), or a sudden weight loss of more than 15% occurred.

2.4. Histopathological observation of pancreatic tissue

Pancreatic tissues, following fixation in 4% paraformaldehyde for 24 h, underwent dehydration through gradient ethanol, clearance in xylene, and embedding in paraffin for the preparation of continuous 4 μm-thick sections. Hematoxylin-eosin (HE) staining was performed as follows: after deparaffinization and rehydration, staining of the sections was performed using hematoxylin for 5 min, followed by blueing under tap water, differentiation in 1% hydrochloric acid ethanol for 30 s, eosin staining for 2 min, dehydration through gradient ethanol, clearing in xylene, and final mounting with neutral balsam. The histopathological changes of pancreatic tissue, including the integrity of acinar structure, the degree of inflammatory cell infiltration, edema, and necrosis, were observed under an upright microscope. The extent of pancreatic injury was quantitatively scored according to the Schmidt scoring criteria, with 5 random high-power fields (×400) selected per section and scored blindly by two pathologists.

The Schmidt pancreatic injury score is assessed in the following four dimensions, with a total score ranging from 0 to 10 points, where a higher score indicates more severe injury.

a. Edema (0–3 points): 0 points, no edema; 1 point, mild interstitial edema; 2 points, moderate interstitial edema with widened acinar spaces; 3 points, diffuse severe edema with pancreatic tissue swelling.
b. Inflammatory cell infiltration (0–3 points): 0 points, no obvious inflammatory cells; 1 point, scattered few inflammatory cells (≤10 per high-power field); 2 points, moderate inflammatory cell infiltration (11–30 per high-power field); 3 points, massive aggregation of inflammatory cells (>30 per high-power field).
c. Acinar structural disruption (0–2 points): 0 points, intact acinar structure; 1 point, partial acinar structural disorder and disintegration (≤50%); 2 points, extensive acinar structural destruction (>50%).
d. Degree of necrosis (0–2 points): 0 points, no necrosis; 1 point, focal necrosis (≤20% of pancreatic tissue); 2 points, large-area necrosis (>20% of pancreatic tissue).

2.5. Detection of related protein expression in pancreatic tissue by WB

Pancreatic tissues stored at −80°C were taken out and subjected to lysis in RIPA lysis buffer supplemented with protease inhibitors at a ratio of tissue weight to lysis buffer of 1:10. The tissues were homogenized on ice until uniform, followed by incubation (4°C, 30 min). The homogenates were centrifuged (12,000 r/min, 15 min), and the supernatants were collected. The protein concentration was determined using the BCA quantification kit, and the concentration was adjusted according to the results. After adding 5 × loading buffer, the proteins were denatured by boiling (100°C, 10 min). 30 μg of denatured protein were subjected to SDS-PAGE, with a concentration gel voltage of 80 V and a separation gel voltage of 120 V. After electrophoresis, transfer was accomplished (200 mA, 90 min). 5% skim milk was adopted for blocking (25°C, 2 h), and first Ab (NICD 1:1000, Hes1 1:1000, SOX9 1:800, NGN3 1:800, Insulin 1:1000, β-actin 1:5000) were applied (4°C, approximately 16 h). The membranes underwent three sequential washes adopting TBST buffer, each lasting 10 min, and HRP-conjugated secondary Ab (1:5000) was applied (25°C, 1 h). An additional three washes were executed. Visualization was achieved utilizing the ECL kit, and the images were captured using a gel imaging system. The expression levels of the target proteins were analyzed by calculating the intensity ratio of the targets to β-actin adopting Image J. The expression level of SP-D protein was detected using SP-D antibody (Abcam, diluted at 1:1000) as the primary antibody, with the remaining procedures being consistent with the detection of the aforementioned target proteins. This detection was used to verify the gene knockout efficiency in SP-D$^{-/-}$ mice and to analyze the temporal expression characteristics of SP-D in the AP model of WT mice.

2.6. Detection of cell differentiation markers in pancreatic tissue by immunohistochemistry

Paraffin-embedded pancreatic tissue sections were deparaffinized and rehydrated, and incubation was executed with 3% H_2O_2 (25°C, 10 min) to block endogenous peroxidase activity. After rinsing with distilled water, the sections were subjected to high-temperature antigen retrieval in 0.01 mol/L citrate buffer (pH 6.0) for 15 min and then allowed to cool to room temperature naturally. 5% BSA was adopted for blocking (25°C, 30 min), and first Ab (SOX9 1:200, NGN3 1:200, Insulin 1:200) were applied (4°C, approximately 16 h). The sections underwent three sequential washes adopting PBS, each lasting 5 min, and HRP-conjugated secondary Ab (1:500) was applied (25°C, 30 min). Following rinsing, color development was performed using DAB substrate, and the next steps were nuclear counterstaining with hematoxylin, blueing under tap water, dehydration through gradient ethanol, clearing in xylene, and final mounting with neutral balsam. PBS was used instead of the first Ab as a negative control. For each section, five randomly chosen high-power fields (×400) were examined, and positive cells were quantified to calculate the positive rate (number of positive cells/total number of cells × 100%).

The expression level of the target protein was assessed using the internationally standard H-score additive scoring method, with the specific calculation equation being:

$$\text{H-score} = (\text{percentage of weakly positive cells} \times 1) + (\text{percentage of moderately positive cells} \times 2) + (\text{percentage of strongly positive cells} \times 3)$$

The total score ranges from 0 to 300, with higher scores indicating stronger protein expression. The percentage of weakly positive cells refers to the proportion of light-yellow positive cells among the total cells, moderately positive cells refer to the proportion of brownish-yellow positive cells, and strongly positive cells refer to the proportion of brown positive cells, with the sum of the three percentages being 100%.

2.7. Detection of glucose metabolism-related indicators

2.7.1. Fasting blood glucose (FBG) measurement

Before cervical dislocation of mice at each time point, the mice were deprived of food for 12 h while maintaining free access to water. FBG levels were determined using a small animal blood glucose analyzer by collecting blood from the tail vein. Each mouse underwent three independent tests, with the mean value derived from the results.

2.7.2. Oral glucose tolerance test (OGTT)

On d 30 after modeling, following a 12-h fast, mice underwent gavage with a 20% glucose solution at 2 g/kg. Blood samples were collected from the tail vein before gavage (0 min) and at 15, 30, 60, and 120 min post-gavage. Blood glucose levels were measured using a blood glucose analyzer to plot glucose tolerance curves and calculate the area under the curve (AUC). The AUC was calculated using the internationally accepted trapezoidal rule, with the equation being: $AUC_{0\text{-}120}$min = 0.25 × FBG + 0.5× (FBG + 15-min blood glucose) × 15 + 0.5× (15-min blood glucose + 30-min blood glucose) × 15 + 0.5× (30-min blood glucose + 60-min blood glucose) × 30 + 0.5× (60-min blood glucose + 120-min blood glucose) × 60. All time units were uniformly converted to min, with blood glucose units in mmol/L, and the final AUC unit was mmol·L^{-1}·min.

2.7.3. Serum insulin level measurement

Serum samples collected at each time point were used to measure insulin levels. The $OD_{450\ nm}$ was measured, and serum insulin concentrations were computed based on the standard curve. The homeostasis model assessment of insulin resistance (HOMA-IR) was computed: HOMA-IR = FBG (mmol/L) × fasting insulin (mU/L)/22.5, to evaluate insulin sensitivity.

2.8. Amylase (AMY) detection

Serum samples were collected at each time point, and the level of AMY was measured by colorimetry. The OD value at 405 nm was determined, and the activity of serum AMY was calculated according to the standard curve (unit: U/L). AMY is a core indicator reflecting the exocrine function of the pancreas.

2.9. Mortality and final number of mice after modeling

The condition of the mice was observed daily after modeling, and mortality was recorded. No deaths were observed in the AG or in the WT-AP-7d and 30 d groups. One mouse in the WT-AP-1d group died at 12 h due to severe edema and respiratory failure, and one mouse in the WT-AP-3d group died at 48 h due to localized pancreatic necrosis and septic shock. Both groups eventually included 9 mice. No deaths were observed in the CG. In the SP-$D^{-}/^{-}$-AP-1d group, two mice died at 8 h due to acute pancreatic necrosis with septic shock and multiple organ failure. In the SP-$D^{-}/^{-}$-AP-3d group, two mice died at 24 h due to pancreatic necrosis with peritoneal infection. In the SP-$D^{-}/^{-}$-AP-7d group, one mouse died at 72 h due to chronic inflammation and suspected malnutrition. The final numbers of mice in these three groups were 8, 8, and 9, respectively. No deaths were observed in the SP-$D^{-}/^{-}$-AP-30d group.

2.10. Statistical processing

All statistical analyses were conducted utilizing SPSS 27.0. Measurement data were reported as mean ± SD (x ± s). Two-way ANOVA was adopted, with genotype (WT/SP-$D^{-}/^{-}$) and treatment (CON/AP) as main effects, and genotype × treatment as the interaction effect. Bonferroni correction was applied for pairwise comparisons. Statistical significance was defined as $p < 0.05$.

3. Results

3.1. Histopathological changes in pancreatic tissue

Histopathological changes in pancreatic tissue were observed by HE staining and quantitatively assessed according to the Schmidt scoring criteria (Table 1). In the AG and CG, pancreatic structures of both WT and SP-$D^{-}/^{-}$ mice were normal at all time points, with Schmidt scores maintained at 0–0.3, and no demonstrable distinctions were noted ($p > 0.05$). In the BG and DG, the degree of injury was evidently more severe in the DG versus the BG at all time points, and the repair process was delayed. At 30 d, in the DG, the total score was still as high as 4.5 ± 0.3, evidently higher than the 1.2 ± 0.2 in the BG ($p < 0.05$). The pancreatic tissue pathological changes were observed by HE staining (Fig. 1). In the AG and CG, the pancreatic acinar structure was intact and regularly arranged at each time point, with no obvious inflammatory infiltration, edema, or necrosis. In the BG, significant acinar structural disorder, edema, and inflammatory cell infiltration were observed at 1 d, with the injury peaking at 3 d, beginning to gradually repair at 7 d, and the acinar structure basically returning to normal at 30 d. In

Table 1
Contrast of Schmidt scores in pancreatic tissue.

Grouping	Time	Edema	Inflammatory cell infiltration	Acinar structural disruption	Necrosis degree	Total score	In contrast to the BG at the same time point (p value)
WT-CON	1 d	0.1 ± 0.1	0.0 ± 0.0	0.0 ± 0.0	0.0 ± 0.0	0.1 ± 0.1	–
	3 d	0.0 ± 0.0	0.1 ± 0.1	0.0 ± 0.0	0.0 ± 0.0	0.1 ± 0.1	–
	7 d	0.1 ± 0.1	0.0 ± 0.0	0.0 ± 0.0	0.0 ± 0.0	0.1 ± 0.1	–
	30 d	0.0 ± 0.0	0.1 ± 0.1	0.0 ± 0.0	0.0 ± 0.0	0.1 ± 0.1	–
WT-AP	1 d	1.8 ± 0.3	2.1 ± 0.2	1.2 ± 0.1	0.9 ± 0.1	6.1 ± 0.4	–
	3 d	1.5 ± 0.2	1.7 ± 0.1	0.9 ± 0.1	0.6 ± 0.1	4.7 ± 0.3	–
	7 d	0.8 ± 0.1	1.0 ± 0.1	0.5 ± 0.1	0.3 ± 0.1	2.6 ± 0.2	–
	30 d	0.3 ± 0.1	0.4 ± 0.1	0.2 ± 0.1	0.3 ± 0.1	1.2 ± 0.2	–
SP-$D^{-}/^{-}$-CON	1 d	0.1 ± 0.1	0.0 ± 0.0	0.0 ± 0.0	0.0 ± 0.0	0.1 ± 0.1	–
	3 d	0.0 ± 0.0	0.1 ± 0.1	0.0 ± 0.0	0.0 ± 0.0	0.1 ± 0.1	–
	7 d	0.1 ± 0.1	0.0 ± 0.0	0.0 ± 0.0	0.0 ± 0.0	0.1 ± 0.1	–
	30 d	0.0 ± 0.0	0.1 ± 0.1	0.0 ± 0.0	0.0 ± 0.0	0.1 ± 0.1	–
SP-$D^{-}/^{-}$-AP	1 d	2.7 ± 0.2	2.8 ± 0.2	1.8 ± 0.1	1.6 ± 0.1	8.9 ± 0.3	<0.05
	3 d	2.5 ± 0.2	2.5 ± 0.1	1.6 ± 0.1	1.5 ± 0.1	8.1 ± 0.2	<0.05
	7 d	1.5 ± 0.2	1.7 ± 0.1	1.2 ± 0.1	0.9 ± 0.1	5.3 ± 0.3	<0.05
	30 d	1.2 ± 0.1	1.3 ± 0.1	0.8 ± 0.1	1.2 ± 0.1	4.5 ± 0.3	<0.05

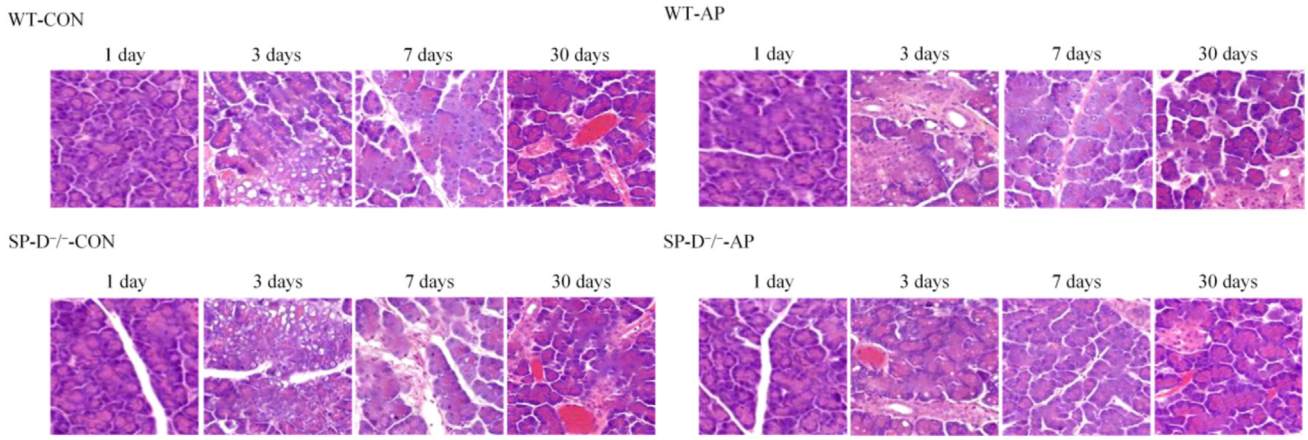

Fig. 1. HE staining results of pancreatic tissue in each group at different time points (×200).

the DG, the injury was more severe than that in the BG at each time point, with obvious acinar structural destruction, inflammatory infiltration, and focal necrosis still present at 30 d, and a significantly delayed repair process.

The mortality rate of the DG was significantly higher than that of the BG: in the BG, 1 death occurred in both the 1-d and 3-d subgroups, with a final count of 9 in each group; whereas in the DG, 2 deaths occurred in the 1-d subgroup, 2 deaths in the 3-d subgroup, and 1 death in the 7-d subgroup, with final counts of 8, 8, and 9, respectively. The higher mortality rate was consistent with the more severe pancreatic pathological damage, further confirming that SP-D deficiency exacerbates the severity of AP and hinders tissue repair.

3.2. Changes in Notch pathway activity

The relative expression (RE) of the key Notch signaling molecules NICD and Hes1 was quantified via WB. The results are presented in Table 2. In the AG and CG, the expression of NICD and Hes1 in both WT and SP-D$^{-/-}$ mice was low and stable, with no demonstrable distinctions ($p > 0.05$). In the BG and DG, NICD and Hes1 in the BG only suggested a transient increase and returned to near-normal levels by d 7. In the DG, both molecules were evidently elevated and remained high, still evidently higher relative to the BG at 30 d ($p < 0.05$).

3.3. Changes in molecules related to acinar cell regeneration

The expression of the ADM marker SOX9 was detected by WB and immunohistochemistry, and the results are shown in Table 3 and Table 4. In the AG and CG, SOX9 expression was low, with no demonstrable distinctions ($p > 0.05$). In the BG and DG, SOX9 expression in the BG first increased and then decreased, reaching a peak at 3 d and gradually returning to normal; SOX9 expression was evidently lower in the DG versus the BG at the identical time ($p < 0.05$). The immunohistochemistry results showed that SOX9-positive cells were mainly localized in the nuclei of acinar cells and ductal-like cells (Fig. 2). In the AG and CG, only a small number of SOX9-positive cells were observed; in the BG, the number of SOX9-positive cells significantly increased at 3 d, mainly concentrated around the damaged areas; in the DG, the number of SOX9-positive cells was significantly lower than that in the BG at the same time point, indicating impaired acinar cell regeneration capacity.

3.4. Changes in molecules related to β-cell regeneration

The expression of the key molecules NGN3 and insulin for β-cell regeneration was detected by WB and immunohistochemistry (Table 5 and Table 6). In the AG and CG, NGN3 expression was always at an extremely low level, and insulin expression was

Table 2
Contrast of RE of NICD and Hes1 in pancreatic tissue.

Grouping	Time	NICD	In contrast to the AG at the identical time (p)	In contrast to the BG at the identical time (p)	Hes1	In contrast to the AG at the identical time (p)	In contrast to the BG at the identical time (p)
WT-CON	1 d	0.2 ± 0.02	–	–	0.1 ± 0.02	–	–
	3 d	0.3 ± 0.02	–	–	0.2 ± 0.02	–	–
	7 d	0.2 ± 0.01	–	–	0.1 ± 0.01	–	–
	30 d	0.3 ± 0.02	–	–	0.2 ± 0.02	–	–
WT-AP	1 d	0.5 ± 0.04	<0.05	–	0.4 ± 0.03	<0.05	–
	3 d	0.4 ± 0.03	<0.05	–	0.3 ± 0.02	<0.05	–
	7 d	0.3 ± 0.02	>0.05	–	0.2 ± 0.02	>0.05	–
	30 d	0.3 ± 0.02	>0.05	–	0.2 ± 0.02	>0.05	–
SP-D$^{-/-}$-CON	1 d	0.2 ± 0.02	>0.05	–	0.1 ± 0.02	>0.05	–
	3 d	0.3 ± 0.02	>0.05	–	0.2 ± 0.02	>0.05	–
	7 d	0.2 ± 0.01	>0.05	–	0.1 ± 0.01	>0.05	–
	30 d	0.3 ± 0.02	>0.05	–	0.2 ± 0.02	>0.05	–
SP-D$^{-/-}$-AP	1 d	0.9 ± 0.05	<0.05	<0.05	0.8 ± 0.04	<0.05	<0.05
	3 d	0.8 ± 0.04	<0.05	<0.05	0.7 ± 0.03	<0.05	<0.05
	7 d	0.6 ± 0.03	<0.05	<0.05	0.5 ± 0.02	<0.05	<0.05
	30 d	0.7 ± 0.03	<0.05	<0.05	0.6 ± 0.03	<0.05	<0.05

Table 3
Contrast of RE of SOX9 in pancreatic tissue.

Grouping	Time	SOX9	Relative to the AG at the identical time (p)	Relative to the BG at the identical time (p)
WT-CON	1 d	0.2 ± 0.02	–	–
	3 d	0.3 ± 0.02	–	–
	7 d	0.2 ± 0.01	–	–
	30 d	0.3 ± 0.02	–	–
WT-AP	1 d	0.5 ± 0.03	<0.05	–
	3 d	0.8 ± 0.04	<0.05	–
	7 d	0.6 ± 0.03	<0.05	–
	30 d	0.3 ± 0.02	>0.05	–
SP-D$^{-/-}$-CON	1 d	0.2 ± 0.02	>0.05	–
	3 d	0.3 ± 0.02	>0.05	–
	7 d	0.2 ± 0.01	>0.05	–
	30 d	0.3 ± 0.02	>0.05	–
SP-D$^{-/-}$-AP	1 d	0.3 ± 0.02	>0.05	<0.05
	3 d	0.4 ± 0.03	<0.05	<0.05
	7 d	0.3 ± 0.02	>0.05	<0.05
	30 d	0.3 ± 0.02	>0.05	>0.05

Table 4
Comparison of immunohistochemistry results for SOX9 in pancreatic tissue.

Grouping	Time	Percentage of positive cells (%)	Staining intensity (weakly/moderately/strongly positive ratio %)	H-score	In contrast to the AG at the identical time (p)	In contrast to the BG at the identical time (p)
WT-CON	1 d	3.2 ± 0.8	3.2/0/0	3.2 ± 0.8	–	–
	3 d	4.1 ± 0.9	4.1/0/0	4.1 ± 0.9	–	–
	7 d	3.5 ± 0.7	3.5/0/0	3.5 ± 0.7	–	–
	30 d	3.8 ± 0.8	3.8/0/0	3.8 ± 0.8	–	–
WT-AP	1 d	18.2 ± 2.1	8.2/10/0	28.2 ± 3.1	<0.05	–
	3 d	35.6 ± 3.2	10.6/20/5	65.6 ± 4.8	<0.05	–
	7 d	22.4 ± 2.5	12.4/10/0	32.4 ± 3.5	<0.05	–
	30 d	6.1 ± 1.0	6.1/0/0	6.1 ± 1.0	>0.05	–
SP-D$^{-/-}$-CON	1 d	3.0 ± 0.7	3.0/0/0	3.0 ± 0.7	>0.05	–
	3 d	3.9 ± 0.8	3.9/0/0	3.9 ± 0.8	>0.05	–
	7 d	3.3 ± 0.6	3.3/0/0	3.3 ± 0.6	>0.05	–
	30 d	3.6 ± 0.7	3.6/0/0	3.6 ± 0.7	>0.05	–
SP-D$^{-/-}$-AP	1 d	8.5 ± 1.2	8.5/0/0	8.5 ± 1.2	>0.05	<0.05
	3 d	15.3 ± 2.0	10.3/5/0	20.3 ± 2.5	<0.05	<0.05
	7 d	10.2 ± 1.5	10.2/0/0	10.2 ± 1.5	>0.05	<0.05
	30 d	5.8 ± 0.9	5.8/0/0	5.8 ± 0.9	>0.05	>0.05

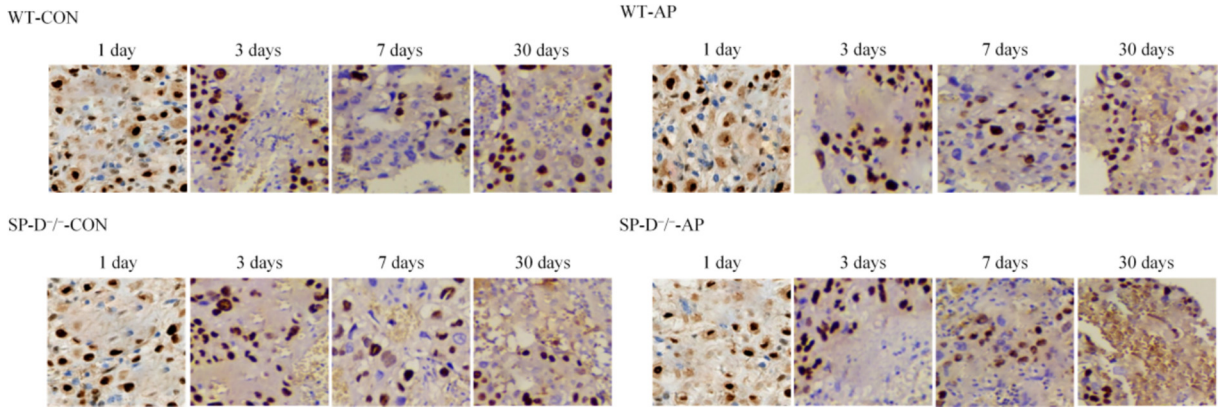

Fig. 2. Immunohistochemical staining results for SOX9 (×200).

stable, with no significant differences between the two groups (p > 0.05). In the BG, NGN3 expression first increased and then decreased, reaching a peak at 3 d and then gradually declining, while insulin expression and serum levels were gradually restored. However, in the DG, NGN3 expression was significantly lower than that in the BG at each corresponding time point, and insulin expression recovered slowly. Even at 30 d, its immunohistochemical H-score and serum levels were still significantly lower than

Table 5
Contrast of RE of NGN3 and Insulin in pancreatic tissue.

Grouping	Time	NGN3	Relative to the AG at the identical time (p)	Relative to the BG at the identical time (p)	Insulin	Relative to the AG at the identical time (p)	Relative to the BG at the identical time (p)
WT-CON	1 d	0.1 ± 0.01	–	–	1.1 ± 0.05	–	–
	3 d	0.2 ± 0.02	–	–	1.2 ± 0.06	–	–
	7 d	0.1 ± 0.01	–	–	1.1 ± 0.05	–	–
	30 d	0.2 ± 0.02	–	–	1.2 ± 0.06	–	–
WT-AP	1 d	0.4 ± 0.03	<0.05	–	0.6 ± 0.04	<0.05	–
	3 d	0.7 ± 0.04	<0.05	–	0.4 ± 0.03	<0.05	–
	7 d	0.5 ± 0.03	<0.05	–	0.7 ± 0.04	<0.05	–
	30 d	0.2 ± 0.02	>0.05	–	0.9 ± 0.05	>0.05	–
SP-D$^{-/-}$-CON	1 d	0.1 ± 0.01	>0.05	–	1.0 ± 0.05	>0.05	–
	3 d	0.2 ± 0.02	>0.05	–	1.1 ± 0.05	>0.05	–
	7 d	0.1 ± 0.01	>0.05	–	1.0 ± 0.04	>0.05	–
	30 d	0.2 ± 0.02	>0.05	–	1.1 ± 0.05	>0.05	–
SP-D$^{-/-}$-AP	1 d	0.2 ± 0.02	>0.05	<0.05	0.5 ± 0.03	<0.05	>0.05
	3 d	0.3 ± 0.02	<0.05	<0.05	0.3 ± 0.02	<0.05	<0.05
	7 d	0.2 ± 0.02	>0.05	<0.05	0.4 ± 0.03	<0.05	<0.05
	30 d	0.2 ± 0.02	>0.05	>0.05	0.5 ± 0.03	<0.05	<0.05

those in the BG ($p < 0.05$), indicating that SP-D deficiency would lead to impaired β-cell regeneration and functional recovery.

3.5. Changes in glucose metabolism-related indicators

FBG, OGTT AUC, and HOMA-IR were measured to evaluate glucose metabolism function (Table 7). In the AG and CG, glucose metabolism indicators were normal, with no demonstrable distinctions ($p > 0.05$). In the BG and DG, glucose metabolism indicators in the BG gradually recovered over time and approached normal levels by d 30. The DG had significantly worse indicators compared to the BG at the same time. The FBG level was still 7.6 ± 0.5 mmol/L at 30 d, and the OGTT AUC was 2110 ± 108 mmol·L^{-1}·min, both significantly higher than those in the BG ($p < 0.05$), indicating delayed recovery of glucose metabolism.

3.6. Changes in pancreatic exocrine and endocrine function indicators

The levels of AMY (an exocrine indicator) and serum insulin (an endocrine indicator) were measured to assess pancreatic function (Table 8). In the AG and CG, the indicators were normal, with no demonstrable distinctions ($p > 0.05$). In the BG and DG, the indicators in the BG returned to normal by d 30; AMY was evidently higher, and insulin was evidently lower in the DG versus the BG, and they did not recover by d 30 ($p < 0.05$).

4. Discussion

Based on the experimental results, in terms of pathological damage, the Schmidt scores were obviously higher in the DG versus the BG (e.g., 4.5 ± 0.3/1.2 ± 0.2 at 30 d), indicating that the absence of SP-D led to more severe tissue edema, inflammatory infiltration, structural disruption, and necrosis, and obviously delayed the repair process. This phenomenon may be related to the loss of control of the inflammatory response following the absence of SP-D as a natural immune regulatory molecule. SP-D can bind to pathogens and apoptotic cells to promote their clearance and regulate macrophage function; its absence may lead to impaired resolution of inflammation and persistent tissue microenvironmental disorders, thereby affecting the regeneration process [12,13]. At the molecular mechanism level, it was found that the absence of SP-D led to abnormally sustained elevation of Notch signaling activity. WB suggested that NICD and Hes1 were obviously higher in the DG versus the BG (e.g., at 30 d, NICD: 0.7 ± 0.03/0.3 ± 0.02; Hes1: 0.6 ± 0.03/0.2 ± 0.02). Moderate activation of the Notch signal helps maintain the pancreatic progenitor cell state and promotes regeneration, but excessive or sustained activation can instead inhibit cell terminal differentiation [14]. The sustained high activity of the Notch signal in the DG in this study may have disrupted the dynamic balance of the regeneration process, causing cells to be arrested in a precursor state and unable to complete differentiation and repair, which was strongly supported by changes in the expression of regeneration markers. Moreover, the regulation of the Notch pathway by SP-D may be achieved by indirectly modulating the inflammatory microenvironment rather than directly binding to Notch signaling molecules. As an innate immune regulatory molecule, SP-D can promote the clearance of apoptotic cells and pathogens by binding to them, regulate macrophage function, and inhibit excessive inflammatory responses. It is hypothesized that during the occurrence of AP, the massive release of inflammatory factors activates the Notch pathway, and the overactivation of the Notch pathway further exacerbates the inflammatory response, creating a vicious cycle. In this study, the pancreatic tissue of the DG had more severe inflammatory infiltration and sustained elevation of inflammatory factor levels, which was indirectly reflected in the significantly higher Schmidt inflammatory infiltration score than that of the BG. This may be an important reason for the sustained activation of the Notch pathway. The presence of SP-D can break the vicious cycle between inflammation and the Notch pathway by inhibiting the excessive release of inflammatory factors, creating a favorable microenvironment for pancreatic cell regeneration. Additionally, SP-D is abnormally expressed in patients with severe AP complicated by acute respiratory distress syndrome and is associated with disease severity, further suggesting the regulatory role of SP-D in inflammation-related pancreatic injury, and its regulation of the Notch pathway may be an extension of its inflammatory regulatory function.

In terms of acinar cell regeneration, SOX9 in the BG peaked at 3 d after injury (0.8 ± 0.04) and then gradually decreased, indicating successful initiation and completion of regeneration; In the DG, SOX9 remained at a low level (0.4 ± 0.03 at 3 d), and the comprehensive immunohistochemical score was also obviously lower (3.1 ± 0.4/7.2 ± 0.5 at 3 d), indicating impaired ADM. ADM is an important regenerative mechanism after pancreatic injury, and SOX9, as a key transcription factor, directly affects the regenerative capacity of acinar cells with insufficient expression [15]. Regarding

Table 6
Contrast of immunohistochemistry results for NGN3 and Insulin in pancreatic tissue.

Grouping	Time	Percentage of NGN3-positive cells (%)	Distribution of NGN3 staining intensity (weakly/moderately/strongly positive ratio %)	NGN3 H-score	Relative to the AG at the identical time (p)	Relative to the BG at the identical time (p)	Percentage of Insulin-positive cells (%)	Distribution of Insulin staining intensity (weakly/moderately/strongly positive ratio %)	Insulin H-score	Relative to the AG at the identical time (p)	Relative to the BG at the identical time (p)
WT-CON	1 d	1.2 ± 0.5	1.2/0/0	1.2 ± 0.5	–	–	32.5 ± 3.0	0/32.5/0	65.0 ± 6.0	–	–
	3 d	1.5 ± 0.6	1.5/0/0	1.5 ± 0.6	–	–	33.8 ± 2.8	0/33.8/0	67.6 ± 5.6	–	–
	7 d	1.3 ± 0.5	1.3/0/0	1.3 ± 0.5	–	–	31.8 ± 2.6	0/31.8/0	63.6 ± 5.2	–	–
	30 d	1.4 ± 0.6	1.4/0/0	1.4 ± 0.6	–	–	32.2 ± 2.7	0/32.2/0	64.4 ± 5.4	–	–
WT-AP	1 d	5.8 ± 1.2	5.8/0/0	5.8 ± 1.2	<0.05	–	20.5 ± 2.2	20.5/0/0	20.5 ± 2.2	<0.05	–
	3 d	12.5 ± 1.8	12.5/0/0	12.5 ± 1.8	<0.05	–	15.3 ± 1.8	15.3/0/0	15.3 ± 1.8	<0.05	–
	7 d	8.6 ± 1.5	8.6/0/0	8.6 ± 1.5	<0.05	–	22.8 ± 2.0	22.8/0/0	22.8 ± 2.0	<0.05	–
	30 d	1.8 ± 0.7	1.8/0/0	1.8 ± 0.7	>0.05	–	28.6 ± 2.5	0/28.6/0	57.2 ± 5.0	>0.05	–
SP-D$^{-/-}$-CON	1 d	1.1 ± 0.4	1.1/0/0	1.1 ± 0.4	>0.05	–	31.8 ± 2.6	0/31.8/0	63.6 ± 5.2	>0.05	–
	3 d	1.4 ± 0.5	1.4/0/0	1.4 ± 0.5	>0.05	–	32.6 ± 2.7	0/32.6/0	65.2 ± 5.4	>0.05	–
	7 d	1.2 ± 0.4	1.2/0/0	1.2 ± 0.4	>0.05	–	31.2 ± 2.5	0/31.2/0	62.4 ± 5.0	>0.05	–
	30 d	1.3 ± 0.5	1.3/0/0	1.3 ± 0.5	>0.05	–	32.0 ± 2.6	0/32.0/0	64.0 ± 5.2	>0.05	–
SP-D$^{-/-}$-AP	1 d	2.5 ± 0.8	2.5/0/0	2.5 ± 0.8	>0.05	<0.05	16.2 ± 1.5	16.2/0/0	16.2 ± 1.5	<0.05	>0.05
	3 d	5.3 ± 1.0	5.3/0/0	5.3 ± 1.0	<0.05	<0.05	10.5 ± 1.2	10.5/0/0	10.5 ± 1.2	<0.05	<0.05
	7 d	3.2 ± 0.9	3.2/0/0	3.2 ± 0.9	>0.05	<0.05	12.8 ± 1.5	12.8/0/0	12.8 ± 1.5	<0.05	<0.05
	30 d	1.6 ± 0.6	1.6/0/0	1.6 ± 0.6	>0.05	>0.05	15.2 ± 1.8	15.2/0/0	15.2 ± 1.8	<0.05	<0.05

β-cell regeneration and functional recovery, NGN3 in the BG transiently increased (0.7 ± 0.04 at 3 d) and then decreased, while Insulin expression and serum levels gradually recovered, approaching normal by d 30 (serum insulin 16.5 ± 1.5 mU/L/17.5 ± 1.5 in the AG). NGN3 in the DG was obviously low (0.3 ± 0.02 at 3 d), indicating impaired differentiation of endocrine precursor cells; Insulin expression and serum levels recovered slowly (serum insulin 12.8 ± 1.2 mU/L at 30 d) [16], and immunohistochemistry showed that both the positive cell rate and comprehensive score were obviously lower than those in the BG (comprehensive score 3.1 ± 0.4/6.2 ± 0.5 at 30 d). The impairment of β-cell regeneration directly led to delayed recovery of glucose metabolism function. Mice in the DG exhibited more severe hyperglycemia, insulin resistance, and impaired glucose tolerance (e.g., at 30 d, FBG 7.6 ± 0.5 mmol/L vs. 5.2 ± 0.3 in the BG; HOMA-IR 1.8 ± 0.1/1.2 ± 0.1), indicating an obviously increased risk of developing diabetes-like metabolic disorders [17]. In addition, the exocrine function indicator AMY was also persistently higher in the DG versus the BG (1480 ± 110 U/L vs. 920 ± 80 at 30 d), further confirming the negative impact of SP-D absence on overall pancreatic repair capacity [18,19].

In summary, SP-D may play a key role in the repair process after AP through modulation of Notch signaling activity. Under normal circumstances, SP-D may inhibit excessive activation of the Notch signal through some mechanism, creating a suitable microenvironment for cell regeneration; however, in the absence of SP-D, the Notch signal is continuously overactive, disrupting the fine regulation of regeneration and differentiation, leading to abnormal expression of SOX9 and NGN3 [20], and ultimately causing impairment of acinar cell and β-cell regeneration [21]. This decline in cell regenerative capacity not only delays histological repair but also leads to delayed recovery of pancreatic exocrine and endocrine functions and the occurrence of glucose metabolism disorders. The protective action of SP-D in preventing the occurrence of post-AP diabetes was revealed at the tissue, cellular, and molecular levels, providing a theoretical basis for SP-D as a potential therapeutic target. Future research can further explore the specific molecular mechanisms by which SP-D directly regulates the Notch signal and the application prospects of improving pancreatic regeneration outcomes by modulating the SP-D-Notch axis through drugs.

Although this study clarified the core role of SP-D in promoting pancreatic injury repair by regulating the activity of the Notch pathway, it still had certain limitations. First, the overexpression model of SP-D was not constructed, and the promoting effect of exogenously increased SP-D expression on the Notch pathway and pancreatic repair could not be directly verified. The necessity of SP-D was only confirmed by the knockout model, and the sufficiency was not verified. Second, the specific molecular mechanism of SP-D regulation of the Notch pathway was not clarified. It could not be determined whether the two interact directly or indirectly through intermediate mediators, nor was it explored whether SP-D affects its activity by binding to Notch pathway-related ligands or receptors. In addition, the specific expression levels of inflammatory factors were not detected in this study, and there was a lack of direct data support.

In response to the above limitations, future research can be carried out in the following directions: Construction of SP-D overexpressing mouse models or conducting SP-D overexpression experiments mediated by adenovirus to verify the improvement effect of exogenous SP-D on the activity of the Notch pathway, pancreatic cell regeneration, and glucose metabolism after AP, providing more direct evidence for clinical application; Adoption of co-immunoprecipitation, luciferase reporter gene and other technologies to explore the interaction between SP-D and key molecules of the Notch pathway or their upstream and downstream regulatory molecules and clarifying the molecular targets of SP-D regulation

Table 7
Contrast of glucose metabolism-related indicators.

Grouping	Time	FBG (mmol/L)	OGTT AUC (mmol·L⁻1·min)	HOMA-IR	Relative to the BG at the identical time (*p*)	Compared with the genotype control group (*p*)
WT-CON	1 d	4.8 ± 0.3	1615 ± 68	1.1 ± 0.1	–	>0.05
	3 d	4.7 ± 0.2	1595 ± 59	1.0 ± 0.1	–	>0.05
	7 d	4.9 ± 0.3	1645 ± 79	1.1 ± 0.1	–	>0.05
	30 d	4.8 ± 0.2	1625 ± 69	1.0 ± 0.1	–	>0.05
WT-AP	1 d	7.2 ± 0.5	2240 ± 118	2.1 ± 0.2	–	<0.05
	3 d	6.5 ± 0.4	2070 ± 109	1.8 ± 0.1	–	<0.05
	7 d	5.8 ± 0.4	1840 ± 98	1.5 ± 0.1	–	<0.05
	30 d	5.2 ± 0.3	1675 ± 78	1.2 ± 0.1	–	>0.05
SP-D⁻/⁻-CON	1 d	4.9 ± 0.3	1635 ± 69	1.1 ± 0.1	–	>0.05
	3 d	4.8 ± 0.2	1605 ± 60	1.0 ± 0.1	–	>0.05
	7 d	5.0 ± 0.3	1655 ± 79	1.1 ± 0.1	–	>0.05
	30 d	4.9 ± 0.2	1635 ± 68	1.0 ± 0.1	–	>0.05
SP-D⁻/⁻-AP	1 d	8.5 ± 0.6	2510 ± 128	2.5 ± 0.2	<0.05	<0.05
	3 d	9.8 ± 0.7	2670 ± 148	2.8 ± 0.2	<0.05	<0.05
	7 d	8.2 ± 0.6	2340 ± 118	2.3 ± 0.2	<0.05	<0.05
	30 d	7.6 ± 0.5	2110 ± 108	1.8 ± 0.1	<0.05	<0.05

Table 8
Contrast of serum AMY and insulin levels.

Grouping	Time	AMY(U/L)	Serum insulin (mU/L)	Relative to the BG at the identical time (*p*)	Relative to the control of the same genotype at the identical time (*p*)
WT-CON	1 d	850 ± 60	16.8 ± 1.3	–	>0.05
	3 d	830 ± 50	17.2 ± 1.4	–	>0.05
	7 d	860 ± 70	16.5 ± 1.2	–	>0.05
	30 d	880 ± 60	17.5 ± 1.5	–	>0.05
WT-AP	1 d	2150 ± 150	8.5 ± 1.0	–	<0.05
	3 d	1820 ± 130	10.2 ± 1.1	–	<0.05
	7 d	1320 ± 120	12.3 ± 1.2	–	<0.05
	30 d	920 ± 80	16.5 ± 1.5	–	>0.05
SP-D⁻/⁻-CON	1 d	860 ± 60	16.5 ± 1.2	–	>0.05
	3 d	840 ± 50	17.0 ± 1.3	–	>0.05
	7 d	870 ± 70	16.8 ± 1.4	–	>0.05
	30 d	890 ± 60	17.2 ± 1.3	–	>0.05
SP-D⁻/⁻-AP	1 d	2580 ± 180	6.2 ± 0.8	<0.05	<0.05
	3 d	2350 ± 160	7.8 ± 0.9	<0.05	<0.05
	7 d	1850 ± 150	9.5 ± 1.0	<0.05	<0.05
	30 d	1480 ± 110	12.8 ± 1.2	<0.05	<0.05

of the Notch pathway; Detection of the expression levels of inflammatory factors in pancreatic tissue and serum; Conducting clinical sample research to detect the expression changes of SP-D, Notch pathway molecules and inflammatory factors in different courses of AP patients and analyzing their correlation with patient prognosis and the risk of post-pancreatitis diabetes to provide a basis for translational medicine research.

5. Conclusions

SP-D has a key protective action in tissue repair and maintenance of metabolic homeostasis after AP. Its mechanism may be related to the regulation of Notch signaling activity: the absence of SP-D leads to sustained activation of the Notch signal, which in turn inhibits the regeneration process of pancreatic acinar and β cells, delays tissue repair and functional recovery, and ultimately increases the risk of diabetes. These findings provide a theoretical basis for SP-D as a potential therapeutic target to prevent the occurrence of post-AP diabetes.

CRediT authorship contribution statement

Jiexin Yan: Writing – original draft. **Shuxiong Liu:** Writing – original draft. **Jian He:** Writing – original draft.

Ethical approval (animals)

All experimental protocols were approved by the Third Affiliated Hospital of Naval Medical University. The experimental procedures were conducted following the National Institutes of Health (NIH) Guidelines for the Protection and Use of Laboratory Animals (NIH Publication No., as per regulations 85-23, updated in 1996). All methods were carried out in accordance with relevant guidelines and regulations. All methods are reported in accordance with ARRIVE guidelines.

Financial support

This research did not receive any specific grant from funding agencies in the public, commercial, or not-for-profit sectors.

Declaration of competing interest

None.

Supplementary material

https://doi.org/10.1016/j.ejbt.2026.100716.

Data availability

The data that support the findings of this study are available from the corresponding author upon reasonable request.

References

[1] Hu C, Chen Y, Yin X, et al. Pancreatic endocrine and exocrine signaling and crosstalk in physiological and pathological status. Signal Transduct Target Ther 2025;10(1):39. https://doi.org/10.1038/s41392-024-02098-3. PMid: 39948335.

[2] Pichardo-Lowden A, Goodarzi MO, Trikudanathan G, et al. Risk and factors determining diabetes after mild, nonnecrotizing acute pancreatitis. Curr Opin Gastroenterol 2024;40(5):396–403. https://doi.org/10.1097/MOG.0000000000001055. PMid: 38935336.

[3] Chernysheva MB, Ruchko ES, Karimova MV, et al. Development, regeneration, and physiological expansion of functional β-cells: Cellular sources and regulators. Front Cell Dev Biol 2024;12:1424278. https://doi.org/10.3389/fcell.2024.1424278. PMid: 39045459.

[4] Ward A, Farengo-Clark D, McKenna DB, et al. Clinical management of TP53 mosaic variants found on germline genetic testing. Cancer Genet 2024;284–285:43–7. https://doi.org/10.1016/j.cancergen.2024.04.002. PMid: 38677009.

[5] Swain S, Narayan RK, Mishra PR. Unraveling the interplay: Exploring signaling pathways in pancreatic cancer in the context of pancreatic embryogenesis. Front Cell Dev Biol 2024;12:1461278. https://doi.org/10.3389/fcell.2024.1461278. PMid: 39239563.

[6] Le N, Vu TD, Palazzo I, et al. Robust reprogramming of glia into neurons by inhibition of Notch signaling and nuclear factor I (NFI) factors in adult mammalian retina PMid: 38996013. Sci Adv 2024;10(28):eadn2091. https://doi.org/10.1126/sciadv.adn2091.

[7] Liu H, Tang T. Pan-cancer genetic analysis of disulfidptosis-related gene set. Cancer Genet 2023;278–279:91–103. https://doi.org/10.1016/j.cancergen.2023.10.001. PMid: 37879141.

[8] Mapindra MP, Castillo-Hernandez T, Clark H, et al. Surfactant Protein-A and its immunomodulatory roles in infant respiratory syncytial virus infection: A potential for therapeutic intervention? Am J Physiol-Lung Cell Mol Physiol 2025;328(1):L179–96. https://doi.org/10.1152/ajplung.00199.2024. PMid: 39662519.

[9] Lv F, Zhou W, Li K. The roles of collectins in renal diseases and transplantation. Immunol Lett 2025;271:106945. https://doi.org/10.1016/j.imlet.2024.106945. PMid: 39542045.

[10] Li X, Zeng Q, Liu C, et al. The immune modulatory role of surfactants in *Mycoplasma pneumoniae* infection. J Inflamm Res 2025;18:2909–22. https://doi.org/10.2147/JIR.S507526. PMid: 40034686.

[11] Guo J, Wu B, Liu Y, et al. Effect of blood purification combined with antibiotics on CC-16 and SP-D levels and prognosis in patients with severe acute pancreatitis complicated by acute respiratory distress syndrome. Am J Transl Res 2025;17(1):429–39. https://doi.org/10.62347/LVRO1003. PMid: 39959207.

[12] Mondal S, Ghanta KP, Bandyopadhyay S. Microscopic understanding of the conformational stability of the aggregated nonamyloid β components of α-synuclein. J Chem Inf Model 2023;63(5):1542–55. https://doi.org/10.1021/acs.jcim.2c01540. PMid: 36866721.

[13] Ou L, Zhu Z, Hao Y, et al. 1,3,6-Trigalloylglucose: A novel potent anti-*Helicobacter pylori* adhesion agent derived from aqueous extracts of *Terminalia chebula* Retz. Molecules 2024;29(5):1161. https://doi.org/10.3390/molecules29051161. PMid: 38474673.

[14] Ahmed I, Mohamed A, Savari O, et al. Expression of DLL3 and SEZ6 in the spectrum of neuroendocrine neoplasia. Endocr Pathol 2025;36(1):27. https://doi.org/10.1007/s12022-025-09873-0. PMid: 40699376.

[15] Liu G, Li Y, Li M, et al. Charting a high-resolution roadmap for regeneration of pancreatic β cells by *in vivo* transdifferentiation from adult acinar cells. Sci Adv 2023;9(21):eadg2183. https://doi.org/10.1126/sciadv.adg2183. PMid: 37224239.

[16] Jiang Y, Yang J, Xia L, et al. Gut microbiota-tryptophan metabolism-GLP-1 axis participates in β-cell regeneration induced by dapagliflozin. Diabetes 2024;73(6):926–40. https://doi.org/10.2337/db23-0553. PMid: 38471012.

[17] Lv B, Liu S, Li Y, et al. Mulberry leaf ameliorate STZ induced diabetic rat by regulating hepatic glycometabolism and fatty acid β-oxidation. Front Pharmacol 2024;15:1428604. https://doi.org/10.3389/fphar.2024.1428604. PMid: 39635431.

[18] Niu X, Sun W, Tang X, et al. Bufalin alleviates inflammatory response and oxidative stress in experimental severe acute pancreatitis through activating Keap1-Nrf2/HO-1 and inhibiting NF-κB pathways. Int Immunopharmacol 2024;142(PartA). https://doi.org/10.1016/j.intimp.2024.113113. PMid: 39276459.

[19] Chvanov M, Voronina S, Jefferson M, et al. Deletion of the WD40 domain of ATG16L1 exacerbates acute pancreatitis, abolishes LAP-like non-canonical autophagy and slows trypsin degradation. Autophagy 2025;21(1):210–22. https://doi.org/10.1080/15548627.2024.2392478. PMid: 39216469.

[20] Zou J, Du C, Liu S, et al. Notch1 signaling regulates Sox9 and VEGFA expression and governs BMP2-induced endochondral ossification of mesenchymal stem cells. Genes Dis 2024;12(3):101336. https://doi.org/10.1016/j.gendis.2024.101336. PMid: 40083323.

[21] Sun J, Wang Y, Fu H, et al. Mettl3-mediated m6A methylation controls pancreatic bipotent progenitor fate and islet formation. Diabetes 2024;73(2):237–49. https://doi.org/10.2337/db23-0360. PMid: 37963393.